

# ADVANCED OPTICAL MATERIALS

## Supporting Information

for *Adv. Optical Mater.*, DOI: 10.1002/adom.202200721

### Reconfigurable Parfocal Zoom Metalens

*Fan Yang, Hung-I Lin, Mikhail Y. Shalaginov, Katherine Stoll, Sensong An, Clara Rivero-Baleine, Myungkoo Kang, Anuradha Agarwal, Kathleen Richardson, Hualiang Zhang, Juejun Hu,\* and Tian Gu\**

# Reconfigurable parfocal zoom metalens: supplemental document

Fan Yang<sup>†</sup> Hung-I Lin<sup>†</sup> Mikhail Y. Shalaginov<sup>†</sup> Katherine Stoll Sensong An Clara Rivero-Baleine Myungkoo Kang Anuradha Agarwal Kathleen Richardson Hualiang Zhang Juejun Hu\* Tian Gu\*

<sup>†</sup>These authors contributed equally to the work.

Fan Yang, Dr. Hung-I Lin, Dr. Mikhail Y. Shalaginov, Katherine Stoll, Dr. Sensong An, Dr. Anuradha Agarwal, Prof. Juejun Hu, Dr. Tian Gu

Department of Materials Science & Engineering, Massachusetts Institute of Technology, Cambridge, MA, USA

Email Address: hujuejun@mit.edu, gutian@mit.edu

Prof. Kathleen Richardson, Dr. Myungkoo Kang

The College of Optics & Photonics, Department of Materials Science and Engineering, University of Central Florida, Orlando, FL, USA

Dr. Clara Rivero-Baleine

Missiles and Fire Control, Lockheed Martin Corporation, Orlando, FL, USA

Prof. Hualiang Zhang

Department of Electrical & Computer Engineering, University of Massachusetts Lowell, Lowell, MA, USA

Dr. Anuradha Agarwal, Dr. Tian Gu

Materials Research Laboratory, Massachusetts Institute of Technology, Cambridge, MA, USA

## 1 Optical responses of the polarization-multiplexed meta-atom structures

We selected 16 meta-atom structures to construct the polarization-multiplexed zoom lens. The structural dimensions, as well as their phase and amplitude responses are listed in Table S1.

## 2 Phase profiles of the polarization-multiplexed zoom metalens

The phase profiles of the metasurfaces were assumed to be even order polynomials forms in both the wide-angle and telephoto modes:

$$\phi(r) = \sum_{i=1}^{11} A_i \left( \frac{r}{R} \right)^{2i} \quad (1)$$

where  $R = 3 \text{ mm}$ ,  $r$  is the radial coordinate, and  $A_i$ 's are the polynomial coefficients. For the front metasurface,  $r_{max} = 0.4 \text{ mm}$  in the wide-angle mode, and  $r_{max} = 0.8 \text{ mm}$  in the telephoto mode. For

Table S1: Polarization-multiplexed meta-atoms

<b>Meta-atom index</b>	<b>1</b>	<b>2</b>	<b>3</b>	<b>4</b>	<b>5</b>	<b>6</b>	<b>7</b>	<b>8</b>
X dimension [nm]	144	132	167	159	190	98	90	90
Y dimension [nm]	144	190	102	113	132	98	125	140
X-pol phase [°]	-2	0	-2	1	86	87	87	97
Y-pol phase [°]	-2	86	182	266	0	87	185	270
X-pol transmittance	0.88	0.87	0.89	0.89	0.70	0.93	0.93	0.91
Y-pol transmittance	0.88	0.70	0.74	0.77	0.87	0.93	0.74	0.77
<b>Meta-atom index</b>	<b>9</b>	<b>10</b>	<b>11</b>	<b>12</b>	<b>13</b>	<b>14</b>	<b>15</b>	<b>16</b>
X dimension [nm]	102	125	236	109	113	140	128	125
Y dimension [nm]	167	90	240	128	159	90	109	125
X-pol phase [°]	182	185	177	180	266	270	267	278
Y-pol phase [°]	-2	87	184	267	1	97	180	278
X-pol transmittance	0.74	0.74	0.78	0.73	0.77	0.77	0.77	0.78
Y-pol transmittance	0.89	0.93	0.74	0.77	0.89	0.91	0.73	0.78

Table S2: Polynomial coefficients of the phase profiles of the polarization-multiplexed zoom metalens

MS-1 wide-angle	$A_1$	$A_2$	$A_3$	$A_4$	$A_5$	$A_6$
	$2.85 \times 10^4$	$1.54 \times 10^4$	$-2.96 \times 10^6$	$7.80 \times 10^9$	$-2.87 \times 10^{12}$	$5.62 \times 10^{14}$
	$A_7$	$A_8$	$A_9$	$A_{10}$	$A_{11}$	
	$-6.50 \times 10^{16}$	$4.56 \times 10^{18}$	$-1.91 \times 10^{20}$	$4.37 \times 10^{21}$	$-4.23 \times 10^{22}$	
MS-1 telephoto	$A_1$	$A_2$	$A_3$	$A_4$	$A_5$	$A_6$
	$-1.87 \times 10^4$	$3.30 \times 10^3$	$9.95 \times 10^4$	$-2.62 \times 10^6$	$1.67 \times 10^7$	$7.31 \times 10^8$
	$A_7$	$A_8$	$A_9$	$A_{10}$	$A_{11}$	
	$-2.10 \times 10^{10}$	$2.47 \times 10^{11}$	$-1.50 \times 10^{12}$	$5.26 \times 10^{12}$	$-1.30 \times 10^{13}$	
MS-2 wide-angle	$A_1$	$A_2$	$A_3$	$A_4$	$A_5$	$A_6$
	$-3.06 \times 10^4$	$4.51 \times 10^4$	$-1.91 \times 10^6$	$4.64 \times 10^7$	$-6.67 \times 10^8$	$6.02 \times 10^9$
	$A_7$	$A_8$	$A_9$	$A_{10}$	$A_{11}$	
	$-3.50 \times 10^{10}$	$1.31 \times 10^{11}$	$-3.04 \times 10^{11}$	$3.99 \times 10^{11}$	$-2.26 \times 10^{11}$	
MS-2 telephoto	$A_1$	$A_2$	$A_3$	$A_4$	$A_5$	$A_6$
	$6.47 \times 10^4$	$1.06 \times 10^6$	$-1.51 \times 10^9$	$7.97 \times 10^{11}$	$-2.55 \times 10^{14}$	$5.11 \times 10^{16}$
	$A_7$	$A_8$	$A_9$	$A_{10}$	$A_{11}$	
	$-6.30 \times 10^{18}$	$4.56 \times 10^{20}$	$-1.79 \times 10^{22}$	$3.78 \times 10^{23}$	$-5.61 \times 10^{24}$	

the back metasurface,  $r_{max} = 2 \text{ mm}$  in both the two modes. The polynomial coefficients were optimized by maximizing the focal spot intensities on the image plane with angle-of-incidences (AOIs) of  $0^\circ$ ,  $10^\circ$ , and  $20^\circ$  in the wide-angle mode, and  $0^\circ$ ,  $1^\circ$ , and  $2^\circ$  in the telephoto mode. The optimized coefficients are listed in Table S2.

### 3 Phase-change reconfigurable meta-atom designs

We carefully engineered the meta-atoms to realize arbitrary phase profiles in both amorphous and crystalline states, in order to achieve the desired functionalities. In ideal cases, the meta-atom designs should have high transmission and individual phase profile tuning ability under both states to fulfil the perfectly accurate phase map targets. However, due to the limited design degrees of freedom, this is impractical. Alternatively, we discretized the full  $2\pi$  phase coverage (which is essential to most optical functionalities) into four 90-degree intervals for each state, so that every point along an arbitrary phase mask will be mapped to one of these four steps. For arbitrary reconfigurability, it is required that for each step in one state, there must be a structure that can assume each of the four steps in the other state. This requires a total of 16 unique structures, which we refer to as a 4-level or 2-bit design. We found an optimal set of meta-atom structures with a lattice constant of  $3 \mu\text{m}$ , and thickness of  $1.1 \mu\text{m}/1.065 \mu\text{m}$  for the amorphous/crystalline state, so that the full  $2\pi$  phase coverage can be achieved under both states. We conducted a thorough parameter sweep, considering three types of resonators including H-shaped (Figure S1a), I-shaped (Figure S1b) and cross-shaped structures (Figure S1c). A sidewall angle of  $85^\circ$  and 3.2% thickness shrinkage (when reconfigured from amorphous to crystalline state) were applied to the meta-atom models during simulation to account for the impact of fabrication and annealing processes. As shown in Figures S1a-c, each meta-atom was modeled using four distinct parameters. For each single meta-atom, unit cell boundary conditions were employed along both x and y axis for the calculation of transmission amplitude and phase. Open boundaries are applied in both the positive and negative z directions. X-polarized incident waves are illuminated from the substrate side and propagate in the z direction. Simulated transmission amplitudes and phases of meta-atoms with different shapes are plotted in Figures S1d-e. Through the combination of these different meta-atom structures, we are able to realize relatively high transmission within the entire  $0-2\pi$  phase range under both amorphous state and crystalline state.

Sets of 16 meta-atoms (i.e. the 2-bit set shown in Figure S1f) that provide full  $2\pi$  phase coverage in both states are selected from the simulation results plotted in Figures S1d-e. These sets can be used in designs to generate arbitrary wavefronts under both amorphous and crystalline states. For each discrete phase under one state, four discrete phases covering  $2\pi$  with about  $90^\circ$  phase intervals could be found

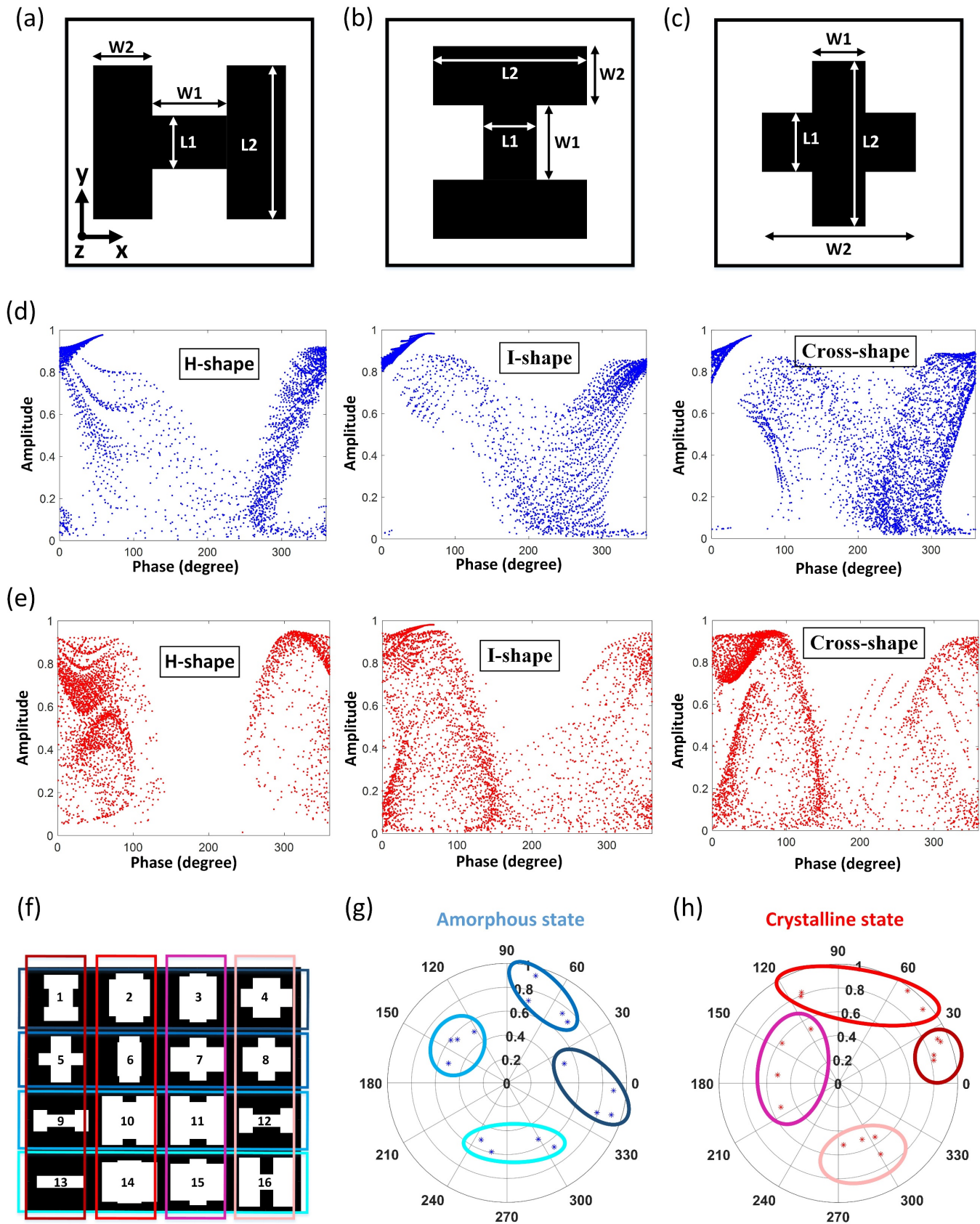


Figure S1: Schematic top-view of an (a) H-shaped, (b) I-shaped and (c) Cross-shaped meta-atom design, with x-polarized incidence. (d)-(e) Scatter diagrams of the transmission phase and amplitude derived with the different shaped meta-atoms shown in (a)-(c), under amorphous state (blue dots, figure (d)) and crystalline state (red dots, figure (e)), respectively. (f) Schematic top-view of all selected 2-bit meta-atom designs; (g) simulated phase and amplitude of the 16 meta-atoms under amorphous state; (h) simulated phase and amplitude of the 16 meta-atoms under crystalline state.

Table S3: Phase-change reconfigurable meta-atoms

Meta-atom index (shape)	1 (I)	2 (+)	3 (+)	4 (+)	5 (+)	6 (+)	7 (+)	8 (+)
$L_1$ [ $\mu m$ ]	1.05	1.8	2.1	0.9	0.6	1.65	1.2	1.2
$W_1$ [ $\mu m$ ]	0.9	1.2	0.75	1.2	0.9	0.9	0.75	0.75
$L_2$ [ $\mu m$ ]	1.5	2.4	2.4	1.95	2.25	2.25	2.1	2.1
$W_2$ [ $\mu m$ ]	0.675	1.8	1.65	2.25	1.95	1.05	2.4	2.1
Amorphous state phase [ $^\circ$ ]	24	22	16	41	117	53	113	112
Crystalline state phase [ $^\circ$ ]	75	162	-103	-18	45	143	-61	-17
Amorphous state transmittance	0.83	0.85	0.70	0.88	0.26	0.94	0.63	0.68
Crystalline state transmittance	0.50	0.27	0.35	0.63	0.52	0.35	0.29	0.83
Meta-atom index (shape)	9 (H)	10 (H)	11 (H)	12 (H)	13 (+)	14 (+)	15 (+)	16 (H)
$L_1$ [ $\mu m$ ]	0.6	1.8	1.8	0.6	0.6	1.875	1.8	0.9
$W_1$ [ $\mu m$ ]	1.2	0.6	0.75	1.2	2.25	1.05	0.75	0.6
$L_2$ [ $\mu m$ ]	1.05	2.4	2.4	1.2	0.6	2.025	2.25	2.55
$W_2$ [ $\mu m$ ]	0.6	0.9	0.825	0.6	2.25	2.4	2.4	0.9
Amorphous state phase [ $^\circ$ ]	-157	-85	144	172	-67	-55.7	14	-59
Crystalline state phase [ $^\circ$ ]	52	123	-54	-4	75	139	-114	19
Amorphous state transmittance	0.27	0.27	0.34	0.26	0.26	0.30	0.68	0.48
Crystalline state transmittance	0.55	0.26	0.44	0.80	0.86	0.30	0.27	0.26

Table S4: Polynomial coefficients of the phase profiles of the phase-change zoom metalens

MS-1 wide-angle	$A_1$	$A_2$	$A_3$	$A_4$	$A_5$	$A_6$
	$1.72 \times 10^3$	$-1.99 \times 10^5$	$5.28 \times 10^7$	$-7.51 \times 10^9$	$6.19 \times 10^{11}$	$-2.91 \times 10^{13}$
	$A_7$	$A_8$	$A_9$	$A_{10}$	$A_{11}$	
	$6.51 \times 10^{14}$	$2.41 \times 10^{15}$	$-4.82 \times 10^{17}$	$1.00 \times 10^{19}$	$-6.94 \times 10^{19}$	
MS-1 telephoto	$A_1$	$A_2$	$A_3$	$A_4$	$A_5$	$A_6$
	$-2.17 \times 10^3$	$-7.25 \times 10^2$	$4.86 \times 10^4$	$-8.06 \times 10^5$	$7.27 \times 10^6$	$-3.59 \times 10^7$
	$A_7$	$A_8$	$A_9$	$A_{10}$	$A_{11}$	
	$8.13 \times 10^7$	$2.77 \times 10^7$	$-5.08 \times 10^8$	$7.92 \times 10^8$	$-2.16 \times 10^8$	
MS-2 wide-angle	$A_1$	$A_2$	$A_3$	$A_4$	$A_5$	$A_6$
	$-3.68 \times 10^3$	$3.30 \times 10^3$	$-8.77 \times 10^4$	$1.47 \times 10^6$	$-1.45 \times 10^7$	$8.05 \times 10^7$
	$A_7$	$A_8$	$A_9$	$A_{10}$	$A_{11}$	
	$-1.97 \times 10^8$	$-2.87 \times 10^8$	$3.20 \times 10^9$	$-7.88 \times 10^9$	$6.79 \times 10^9$	
MS-2 telephoto	$A_1$	$A_2$	$A_3$	$A_4$	$A_5$	$A_6$
	$7.25 \times 10^3$	$-4.68 \times 10^5$	$1.17 \times 10^8$	$-1.83 \times 10^{10}$	$1.55 \times 10^{12}$	$-5.75 \times 10^{13}$
	$A_7$	$A_8$	$A_9$	$A_{10}$	$A_{11}$	
	$-1.12 \times 10^{15}$	$2.08 \times 10^{17}$	$-8.85 \times 10^{18}$	$1.73 \times 10^{20}$	$-1.33 \times 10^{21}$	

at another state. More specifically, in Figure S1f, phase responses of meta-atoms that are circled in red (e.g. meta-atoms or cells #1, 5, 9 and 13) are similar under crystalline state, but are distributed in the  $2\pi$  range with a  $90^\circ$  interval under amorphous state. Meta-atoms that are circled in blue (e.g. meta-atoms #13, 14, 15 and 16) are similar under amorphous states and different under crystalline state. Complete dimensions of these 16 selected meta-atoms, and their phase and amplitude responses are listed in Table S3. All of the listed dimensions refer to the bottom surface of the GSST meta-atoms. The dimensions at the top surface are slightly smaller due to the meta-atom sidewalls slanted at  $85^\circ$ .

#### 4 Phase profiles of the phase-change reconfigurable zoom metalens

Similar to the polarization-multiplexed metalens, the phase profiles of the phase-change metalens were assumed to be even order polynomials forms in both the wide-angle and telephoto modes:

$$\phi(r) = \sum_{i=1}^{11} A_i \left(\frac{r}{R}\right)^{2i} \quad (2)$$

---

where  $R = 3 \text{ mm}$ ,  $r$  is the radial coordinate, and  $A_i$ 's are the polynomial coefficients. For the front metasurface,  $r_{max} = 0.5 \text{ mm}$  in the wide-angle mode, and  $r_{max} = 1.5 \text{ mm}$  in the telephoto mode. For the back metasurface,  $r_{max} = 2 \text{ mm}$  in both the two modes. The optimized coefficients are listed in Table S4.